2011-04-29

# {beta}3GnT2 Maintains Adenylyl Cyclase-3 Signaling and Axon Guidance Molecule Expression in the Olfactory Epithelium

Timothy R. Henion
*University of Massachusetts Medical School*

*Et al.*

Development/Plasticity/Repair

# β3GnT2 Maintains Adenylyl Cyclase-3 Signaling and Axon Guidance Molecule Expression in the Olfactory Epithelium

**Timothy R. Henion, Ashley A. Faden, Thomas K. Knott, and Gerald A. Schwarting**
Department of Cell Biology, University of Massachusetts Medical School, Worcester, Massachusetts 01655

**In the olfactory epithelium (OE), odorant receptor stimulation generates cAMP signals that function in both odor detection and the regulation of axon guidance molecule expression. The enzyme that synthesizes cAMP, adenylyl cyclase 3 (AC3), is coexpressed in olfactory sensory neurons (OSNs) with poly-*N*-acetyllactosamine (PLN) oligosaccharides determined by the glycosyltransferase β3GnT2. The loss of either enzyme results in similar defects in olfactory bulb (OB) innervation and OSN survival, suggesting that glycosylation may be important for AC3 function. We show here that AC3 is extensively modified with *N*-linked PLN, which is essential for AC3 activity and localization. On Western blots, AC3 from the wild-type OE migrates diffusely as a heavily glycosylated 200 kDa band that interacts with the PLN-binding lectin LEA. AC3 from the *β3GnT2*$^{-/-}$ OE loses these PLN modifications, migrating instead as a 140 kDa glycoprotein. Furthermore, basal and forskolin-stimulated cAMP production is reduced 80–90% in the *β3GnT2*$^{-/-}$ OE. Although AC3 traffics normally to null OSN cilia, it is absent from axon projections that aberrantly target the OB. The cAMP-dependent guidance receptor neuropilin-1 is also lost from *β3GnT2*$^{-/-}$ OSNs and axons, while semaphorin-3A ligand expression is upregulated. In addition, kirrel2, a mosaically expressed adhesion molecule that functions in axon sorting, is absent from *β3GnT2*$^{-/-}$ OB projections. These results demonstrate that PLN glycans are essential in OSNs for proper AC3 localization and function. We propose that the loss of cAMP-dependent guidance cues is also a critical factor in the severe axon guidance defects observed in *β3GnT2*$^{-/-}$ mice.**

## Introduction

The orderly convergence of sensory axons to the olfactory bulb (OB) is critical for odor discrimination and processing by the brain. Although the populations of olfactory sensory neurons (OSNs) expressing a given odorant receptor (OR) are widely dispersed in the nasal cavity, their axons converge to form synapses in glomeruli at relatively stereotyped loci in the OB. A critical role for ORs in olfactory axon guidance has long been appreciated, although the mechanism by which they influence targeting has been elusive (Mombaerts et al., 1996; Wang et al., 1998; Feinstein and Mombaerts, 2004). Recently, several studies have convincingly shown that OR-derived cAMP signals are essential for proper olfactory map formation (Imai et al., 2006, 2009; Chesler et al., 2007).

Olfactory signaling proteins are concentrated in specialized cilia that project from OSNs into the nasal lumen (for review, see Jenkins et al., 2009). Odorant binding to ORs activates the $G_{\alpha}s$ homolog $G_{olf}$, which stimulates cAMP production by adenylyl cyclase 3 (AC3). Increased cAMP levels activate a heterotetrameric olfactory cyclic nucleotide gated channel leading to membrane depolarization and the propagation of action potentials (Kleene, 2008) (for review, see Kaupp, 2010). Blocking OR stimulation of AC3 in transgenic mice by disrupting G protein coupling results in a failure of axon convergence (Imai et al. 2006).

A number of molecules associated with cell adhesion and axon guidance are differentially regulated by cAMP (Imai et al., 2006; 2009). Nrp1 is mosaically expressed by subsets of OSNs in the olfactory epithelium (OE) and is required for proper glomerular targeting through interactions with semaphorin-3A (Sema3A) (Schwarting et al., 2000, 2004; Taniguchi et al., 2003). Higher Nrp1 expression is positively correlated with increased cAMP levels, and either downregulating or upregulating Nrp1 in transgenic mice shifts the position of glomeruli toward the anterior or posterior OB, respectively (Imai et al., 2006, 2009). These results are further supported by analysis of AC3 null mice, which exhibit a loss of Nrp1 expression, severely disorganized glomeruli, and anosmia (Wong et al., 2000; Trinh and Storm, 2003; Chesler et al., 2007; Dal Col et al., 2007, Zou et al., 2007).

Interestingly, the effects of AC3 loss mirror the defects we observed in null mice for β3GnT2 (Zhou et al., 1999; Shiraishi et al., 2001), a glycosyltransferase highly expressed by OSNs and other sensory neuron populations (Henion et al., 2005; Schwarting and Henion, 2007). *β3GnT2*$^{-/-}$ mice display a loss of selected OSN subsets and glomeruli, a severe axon pathfinding defect, and impaired sexual behavior (Henion et al., 2005; Biellmann et al., 2008). Here we investigate the relationship between β3GnT2 and olfactory signaling. We show that β3GnT2 has a

Received Jan. 13, 2011; revised Feb. 25, 2011; accepted March 15, 2011.

Author contributions: T.R.H. and G.A.S. designed research; T.R.H., A.A.F., and T.K.K. performed research; T.R.H., A.A.F., T.K.K., and G.A.S. analyzed data; T.R.H. wrote the paper.

This work was supported by National Institutes of Health Grants DC00953 and DC09034 to G.A.S and by the Mizutani Foundation for Glycoscience. We are grateful to Thierry Hennet for providing *β3GnT2*$^{-/-}$ mice used throughout this study, James Schwob for NeuroD1 and Ngn1 cDNAs, Karina Meiri for anti-GAP-43 antibody, Frank Margolis for anti-OMP, Kensaku Mori for anti-OCAM, Brian Nasipak and Chandrashekara Mallappa for helpful discussions regarding qPCR analysis, and Jean Underwood for confocal expertise. We also thank Daniel Storm for reading this manuscript.

Correspondence should be addressed to either Timothy R. Henion or Gerald A. Schwarting, Department of Cell Biology, University of Massachusetts Medical School, 55 Lake Avenue North, Worcester, MA 01655, E-mail: gerald.schwarting@umassmed.edu or timothy.henion@umassmed.edu.

DOI:10.1523/JNEUROSCI.0224-11.2011

 0270-6474/11/316576-11$15.00/0

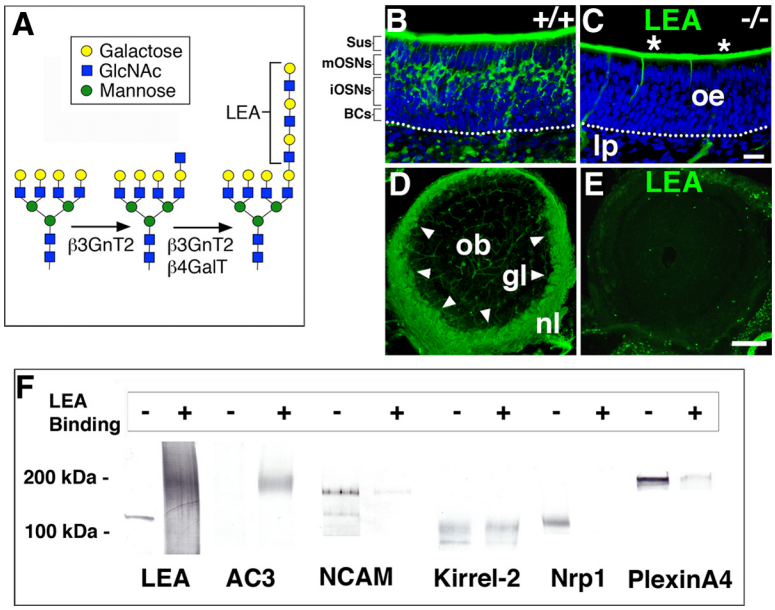


**Figure 1.** PLN glycans are regulated by β3GnT2 in the OE. ***A***, Schematic depicting the role of β3GnT2 in PLN synthesis. The disaccharide *N*-acetyllactosamine (Galβ1–4GlcNAc) can occur on glycoproteins as a single moiety or as a polymer of tandemly repeated (Galβ1–4GlcNAcβ1–3$_n$)-R units. β3GnT2 can both initiate PLN synthesis and, in concert with widely expressed β1,4-galactosyltransferase enzymes (β4GalT), extend these into chains of variable length. LEA lectin is specific for PLN and does not recognize single *N*-acetyllactosamine units. ***B***, ***C***, LEA lectin histochemistry of PD3 mouse OEs. LEA (green) recognizes PLN glycans expressed by mature OSNs in the apical OE (oe) of WT but not *β3GnT2*$^{-/-}$ mice. Nuclei are labeled with Draq5 (blue). The cellular layers of the OE are noted to the left: Sus, Sustentacular cells; mOSNs, mature OSNs; iOSNs, immature OSNs; BCs, basal cell progenitors. Asterisks denote mucin-associated reactivity that is not β3GnT2 dependent. Dotted line demarcates the border between the OE and the underlying lamina propria (lp). Scale bar, 25 μm. ***D***, ***E***, LEA lectin histochemistry of PD3 OBs. LEA strongly labels all axons in the WT OB (ob) nerve layer (nl) and protoglomeruli (gl, arrowheads) with uniform intensity. In contrast, axons in the null OB are unlabeled at all ages. Scale bar, 200 μm. ***F***, Western blot analysis of olfactory glycoproteins fractionated into LEA bound (+) and unbound (−) fractions. AC3 is heavily modified by PLN and segregates exclusively into the LEA bound fraction. Kirrel2, plexin-A4 and NCAM are partially modified by PLN glycans, whereas Nrp1 is not.

novel function in regulating the expression of poly-*N*-acetyllactosamine (PLN) glycans on AC3 that are required for cAMP synthesis. The loss of AC3 activity in *β3GnT2*$^{-/-}$ mice leads to a misregulation of both Nrp1 and Sema3A expression. Our results suggest that PLN glycans are required for maintaining cAMP signaling in olfactory and perhaps other sensory neuron populations.

## Materials and Methods

*Animals.* *β3GnT2*$^{-/-}$ mice were established from the gene-trapped KST308 embryonic stem (ES) cell line, developed through the BayGenomics project (Mitchell et al., 2001). Details of the ES insertion event and generation of *β3GnT2*$^{-/-}$ mice have been reported previously (Henion et al., 2005). Mice were housed according to standard National Institutes of Health and institutional care guidelines, and procedures were approved by the University of Massachusetts Medical School Institutional Animal Care and Use Committee (Worcester, MA).

*Antibodies and lectins.* LEA (*Lycopersicon esculentum*) lectin, biotinylated and Texas Red and FITC conjugated, were obtained from Vector Laboratories. Antibodies used included rabbit anti-AC3 (Santa Cruz Biotechnology), rabbit anti-activated caspase-3 (Cell Signaling Technology), goat anti-actin (Santa Cruz Biotechnology), goat anti-kirrel2 (R & D Systems), mouse anti-neural cell adhesion molecule (NCAM; Sigma-Aldrich), rabbit anti-neuropilin-1 (R & D Systems), and rabbit anti-plexin-A4 (Santa Cruz Biotechnology). Mouse anti-GAP-43 was a gift from Karina Meiri, Tufts University, Boston, MA. Rabbit anti-OCAM was a gift from K. Mori, University of Tokyo, Tokyo, Japan. Goat anti-olfactory marker protein (OMP) was a gift from Frank Margolis, University of Maryland, Baltimore, MD.

*Histology and immunocytochemistry.* For most immunocytochemical procedures, tissues were prepared by transcardial perfusion using 4% paraformaldehyde fixation in 0.1 M PBS, pH 7.4. For Nrp1 labeling, tissues were fixed in 2% paraformaldehyde-lysine-periodate. Heads were subsequently removed and postfixed overnight in the same fixative solution, followed by cryoprotection in 30% sucrose. After embedding, tissue sections were prepared on a Microm HM505E cryostat at 50 μM thickness and then immediately thawed in Transwell boats filled with PBS for staining as free-floating sections. Tissues were blocked for 1 h in 2% BSA and then incubated overnight at 4°C with primary antibodies diluted in 1% BSA/PBS/0.3% Triton X-100. After washing, tissue sections were further incubated for 2 h at room temperature with species-specific secondary antibodies conjugated to either Alexa Fluor 488, Alexa Fluor 568 (1:1000; Invitrogen Corporation), or Cy3 (1:300; Jackson ImmunoResearch Laboratories). Images were captured using either a Leica SP1 laser scanning confocal microscope, or a Zeiss Axioplan photomicroscope equipped with a Spot RT camera (Diagnostic Instruments).

*Cell counts.* AC3-expressing OSNs in postnatal day (PD)3 and adult OEs of *β3GnT2*$^{-/-}$ and wild-type (WT) control mice were quantified from digital images of the dorsal septum. Three mice at each time point were analyzed using five images captured per mouse from sections located near the midpoint OE along the anterior–posterior axis. The number of immunoreactive OSNs was counted for three boxes digitally placed on each image, and the results expressed as the average number of AC3$^+$ OSNs per 50 μM segment of OE. Statistical analysis was performed using SigmaStat 2.0 software.

*Biochemical analyses.* Olfactory epithelia from adult mice between the ages of 6 and 10 weeks of age were carefully removed under a dissecting microscope and homogenized in PBS containing 1% Triton X-100 and a protease inhibitor cocktail (Sigma-Aldrich). OE preparations are comprised mainly of OSNs and other OE cell types, but also contain an adjacent extracellular matrix that includes olfactory axons and blood vessels. Protein concentrations were determined colorimetrically using a BCA protein assay kit (Pierce Biotechnology). Proteins were separated by gradient (4–15%) SDS-PAGE under reducing conditions and transblotted to 0.45 μM nitrocellulose filters. The blots were exposed to primary antibody overnight at 4°C and then to horseradish peroxidase-conjugated secondary antibodies (1:500) for 2 h at room temperature. Immunoreactive bands were visualized using an Opti-4CN substrate kit (Bio-Rad). For enzyme treatment of proteins, 5 μl denaturing solution (0.2% SDS and 100 mM 2-mercaptoethanol) was added to ~100 μg of protein in 50 μl of PBS and heated at 100°C for 10 min. Triton X-100 concentration was adjusted to 1.25%, and 5 U of peptide *N*-glycosidase (PNGase F) (Sigma-Aldrich) was added and incubated at 37°C for 3 h. The reaction was stopped by heating at 100°C for 5 min. Deglycosylation was assessed by change in mobility by SDS-PAGE.

*Affinity purification of PLN-modified glycoproteins.* To fractionate olfactory glycoproteins, freshly dissected OEs were homogenized in 0.1 M Tris-buffered saline, pH 7.5, containing 1.0 mM $CaCl_2$, 1.0 mM $MgCl_2$, 0.5% Nonidet P-40, 5 mM sodium deoxycholate, and protease inhibitor cocktail (Sigma-Aldrich). The homogenate was centrifuged at 12,000 × *g* for 10 min and the protein concentration was adjusted to 6–10 mg/ml. LEA-agarose (200 μl) was equilibrated in homogenization buffer, and then 2 ml of protein was added followed by end-over-end mixing for 4 h at room temperature. The agarose gel was spun at low speed followed by

removal of the supernatant, and the gel was washed three times in homogenization buffer without detergent. The LEA-agarose gel was then mixed end over end at room temperature in TBS containing 0.3 M lactose and protease inhibitors. The resulting supernatant was concentrated to 100 μl using a Centicon-10 spin column (Millipore) for Western blot analysis.

*Real time reverse transcriptase quantitative PCR.* OEs from 3- to 6-month-old WT and *β3GnT2*$^{-/-}$ mice ($n = 3$ for each age and genotype) were microdissected directly into TRIzol reagent (Invitrogen). Total RNA was isolated individually from each sample according to the manufacturer's protocol, and 3 μg of each RNA sample was reverse transcribed into cDNA with random hexamers using the SuperScript II RT System (Invitrogen). Oligonucleotides for quantitative PCR (qPCR) amplification were designed using Primer3 software (version 0.4.0) and are available upon request. qPCRs were set up in triplicate with GoTaq PCR Master Mix (Promega) for amplification on a StepOnePlus Real-Time PCR System (Applied Biosystems). Relative expression levels, normalized to RNA polymerase 2, were determined from comparative $C_T$ (threshold cycle) values calculated using StepOne Real-Time PCR Software.

*Adenylyl cyclase enzyme assays and cAMP immunoassay.* For the analysis of adenylyl cyclase enzymatic activity, OE tissues from PD9 and adult β3GnT2 WT and null mice were carefully microdissected and placed into 0.5 ml of chilled homogenization buffer containing 50 mM Tris-HCl, pH 7.4, 2 mM $MgCl_2$, 1 mM EDTA, 0.5 mM DTT, and 1× protease inhibitor cocktail (Roche). Samples were ground by hand using 20 strokes with a Potter–Elverhejam tissue homogenizer (Kontes), followed by a 7 min centrifugation step at 800 × *g* to pellet debris. Supernatants were further centrifuged at 120,000 × *g* in a Beckman Ultracentrifuge using a SW55Ti rotor. Pellets were resuspended in 0.25 ml homogenization buffer with protease inhibitors and were subsequently ground again by hand using 10 strokes in a tissue homogenizer. Samples were immediately frozen on dry ice and stored at −80°C. Protein concentrations were determined by the BCA Protein Assay Kit (Pierce). For assaying adenylyl cyclase activity, 7 μg of olfactory homogenate was preincubated on ice in 25 μl of homogenization buffer supplemented with 0.5 mM 1-methyl-3-isobutylxanthine to inhibit phosphodiesterase activity. Olfactory homogenates were then supplemented with 100 μl of reaction mix containing 40 mM Tris, pH 7.4, 5 mM $MgCl_2$, 1 mM ATP, 10 mM phosphocreatine, 40 U/ml creatine phosphokinase, 1 mM DTT, 1 mM EDTA, 0.2 mM EGTA, 0.1% BSA, and 10 μM GTP. In addition, stimulated samples were coincubated with 10 μM forskolin, while basal samples received DMSO solvent alone. Reactions were incubated at 37°C for 15 min and then were stopped by boiling for 10 min. The reaction products were homogenized in 7.5% ice-cold TCA, pelleted at 2000 × *g* for 10 min, extracted four times in water-saturated diethyl ether, and dried in a Speed Vac. The amount of cAMP generated in each reaction was quantified by competitive immunoassay using the cAMP Enzyme Immunoassay Kit according to the manufacturer's protocol (CA201, Sigma-Aldrich). Three WT and null mouse OE samples were assayed in duplicate. The immunoassay was repeated three times and the results, expressed as picomoles of cAMP generated per milligram per minute, were averaged for each genotype. The accumulation of cAMP in OE samples at time 0 was negligible and was omitted from further analysis.

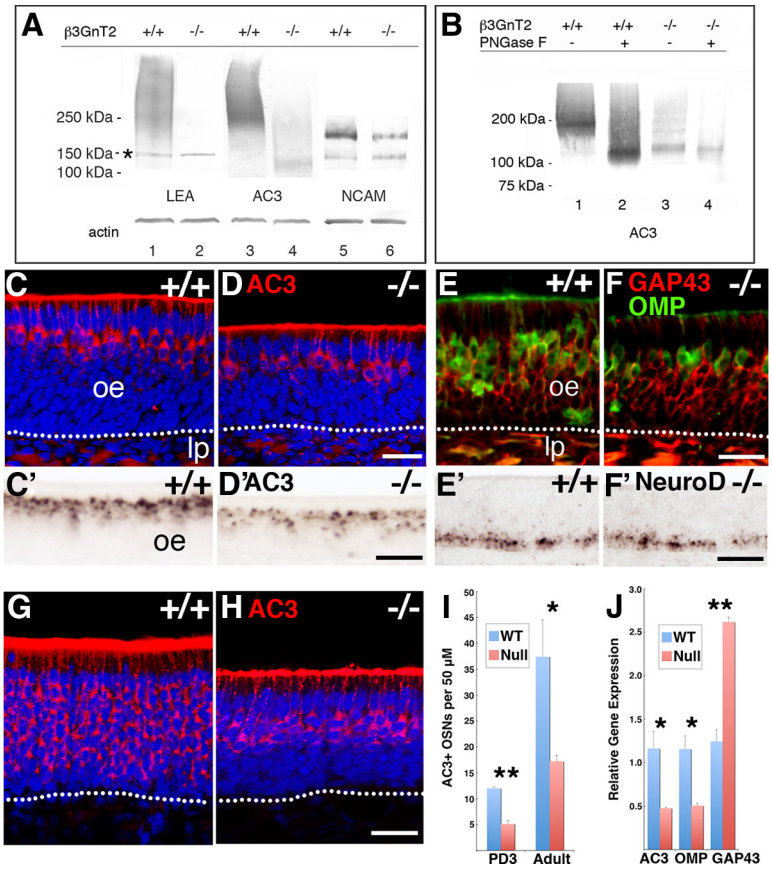


**Figure 2.** β3GnT2 deletion leads to a loss of mature OSNs. ***A***, LEA lectin reacts with heterogeneously migrating glycoproteins in the OE of WT, but not *β3GnT2*$^{-/-}$ mice. AC3 is heavily modified by glycans that reduce its mobility on SDS-PAGE gels. The large shift in mobility for AC3 in null OEs demonstrates that this glycosylation is β3GnT2 dependent. In contrast, a much smaller proportion of the NCAM-180 isoform is glycosylated by β3GnT2. The asterisk denotes a band from nonspecific avidin–biotin binding. ***B***, Western blot analysis of PNGase F-treated OE homogenates from WT and *β3GnT2*$^{-/-}$ mice, confirming that AC3 glycosylation is *N*-linked. The small shift in mobility of PNGase F-treated AC3 in null mice represents the loss of residual core glycans that may be important for protein folding and transport. ***C***, ***D***, Mature OSNs that are immunoreactive for AC3 (red) are reduced in number in the OE (oe) of PD3 *β3GnT2*$^{-/-}$ mice. Dashed line separates the OE from the underlying lamina propria (lp). Nuclei are stained with Draq5 (blue). Scale bar, 25 μm. ***C′***, ***D′***, *In situ* hybridization analysis reveals a similar decrease in *AC3* mRNA, suggesting that the number of mature OSNs, and not just AC3 protein, is reduced in *β3GnT2*$^{-/-}$ mice. Scale bar, 50 μm. ***E***, ***F***, The number of OMP$^{+}$ mature OSNs is decreased in PD3 null mice, while neurons expressing the immature OSN marker GAP-43 are increased. Scale bar, 25 μm. ***E′***, ***F′***, Neural precursors expressing *NeuroD1* are unchanged in null mice relative to WT controls. Scale bar, 50 μm. ***G***, ***H***, The loss of AC3-immunoreactive OSNs persists in the adult OE of *β3GnT2*$^{-/-}$ mice. Scale bar, 25 μm. ***I***, Cell counts for AC3$^{+}$ OSNs at time points depicted in ***C***, ***D***, ***G***, and ***H***. Statistics: Student's *t* test, $^{**}p < 0.001$, $^{*}p < 0.05$, mean ± SEM (PD3 $n = 4$, adult $n = 3$). ***J***, Real-time PCR quantification of relative expression levels for *AC3* and stage-specific markers of OSN differentiation, as detailed in ***C***–***F***. The loss of *OMP* expression in the *β3GnT2*$^{-/-}$ OE parallels that of *AC3*, while *GAP-43* mRNA is increased, further indicating that neural precursors are not depleted in null mice. Statistics: Student's *t* test, $^{**}p < 0.001$, $^{*}p < 0.05$, mean ± SEM ($n = 3$).

In situ *hybridization.* Tissue sections for *in situ* hybridization were fixed in 4% paraformaldehyde as described (see above, Histology and immunocytochemistry) and then sectioned at 14–20 μM thickness before thaw mounting on Superfrost Plus slides (Fisher Scientific). Riboprobes were transcribed with SP6 or T7 polymerase from linearized cDNAs in the presence of digoxigenin labeling mix (Roche). Tissue sections were hybridized to antisense riboprobes and localized with alkaline phosphatase-conjugated anti-digoxigenin antibody (Roche), as detailed previously (Henion et al., 2001). The color reaction was developed with NBT/BCIP (nitro blue tetrazolium and 5-bromo-4-chloro-3-indoyl phosphate) substrate (Roche).

## Results

### PLN expression by olfactory glycoproteins

We have previously reported that the glycosyltransferase β3GnT2 (formerly termed β3GnT1 under a prior nomenclature

by Henion et al., 2005) is required in mice for establishing proper axon connectivity with the OB. The loss of β3GnT2 in OSNs leads to a postnatal delay in OB innervation, axon guidance errors, and multiple abnormalities in glomerular formation that affect all OSN subsets. Terminal *N*-acetyllactosamine moieties recognized by the monoclonal antibody 1B2 are one form of glycan that is decreased in subpopulations of OSNs in *β3GnT2*$^{-/-}$ mice. The widespread nature of the axon guidance defects we observed in null mice as well as the broad distribution of β3GnT2 in the OE led us to examine whether other glycan structures were affected by the absence of this glycosyltransferase.

β3GnT2 both initiates *N*-acetyllactosamine synthesis and extends these structures into large poly-*N*-acetyllactosamine chains of variable length (Fig. 1*A*). These oligosaccharides can be identified in tissues by the lectin *Lycopersicon esculentum* agglutinin, LEA, which binds with high affinity to PLN glycans bearing three or more linear *N*-acetyllactosamine repeats (Merkle and Cummings, 1987). Beginning in embryonic development, mature OSNs strongly bind LEA, as do their axons in the underlying lamina propria and OB (Fig. 1*B*,*D*). However, PLN glycans are absent from OSN cell bodies and OB projections of *β3GnT2*$^{-/-}$ mice (Fig. 1*C*,*E*). These results are consistent with the known activity of β3GnT2 in PLN synthesis (Shiraishi et al., 2001; Zhou et al., 1999; Togayachi et al., 2007) and with the fact that this glycosyltransferase is the only β3GnT family member that is expressed at high levels in the OE (data not shown).

Proper OB targeting is dependent on several guidance molecules expressed on axons whose transcription is regulated by cAMP levels determined by AC3 (Imai et al., 2006, 2009; Chesler et al., 2007; Dal Col et al., 2007; Zou et al. 2007). Similarities between the guidance defects observed in *AC3*$^{-/-}$ *and β3GnT2*$^{-/-}$ mice prompted us to investigate whether PLN might influence AC3 expression and/or function. For this analysis, we first examined whether AC3 and other olfactory guidance receptors were PLN modified. Homogenates from adult OE were first separated into bound and unbound fractions on LEA-agarose before being subjected to Western blot analysis. Greater than 95% of total OE protein separates into the LEA unbound fraction (data not shown). The subset of LEA bound proteins is visible as an extended smear composed of glycoproteins of widely varying molecular weights (Fig. 1*F*).

Prior studies have shown that AC3 expressed by OSNs is a heavily *N*-glycosylated protein that migrates diffusely as a high molecular weight band (Bakalyar and Reed, 1990; Wei et al., 1998). Differences in PLN chain length and composition could be one source of this size heterogeneity. Consistent with this, virtually all AC3 protein is found in the LEA bound fraction, indicating the presence of extensive PLN modifications (Fig. 1*F*). The alternatively spliced NCAM-140 and NCAM-180 isoforms express PLN at different levels. A portion of NCAM-180 binds LEA while NCAM-140 is unbound, suggesting that the six potential extracellular *N*-linked glycosylation sites shared by both isoforms are differentially modified.

We identified several additional OSN glycoproteins that are PLN modified. Kirrel2, a 74 kDa adhesion molecule implicated in homotypic axon sorting (Serizawa et al., 2006), migrates predominantly as a broad 100 kDa band that is retained on LEA-agarose (Fig. 1*F*). In contrast, Nrp1, the glycoprotein receptor for the secreted guidance cue Sema3A, does not bind to LEA-agarose, although a portion of its signaling coreceptor, plexin-A4, is retained. Thus, several adhesion and signaling molecules that influence olfactory axon targeting are modified with PLN glycans.

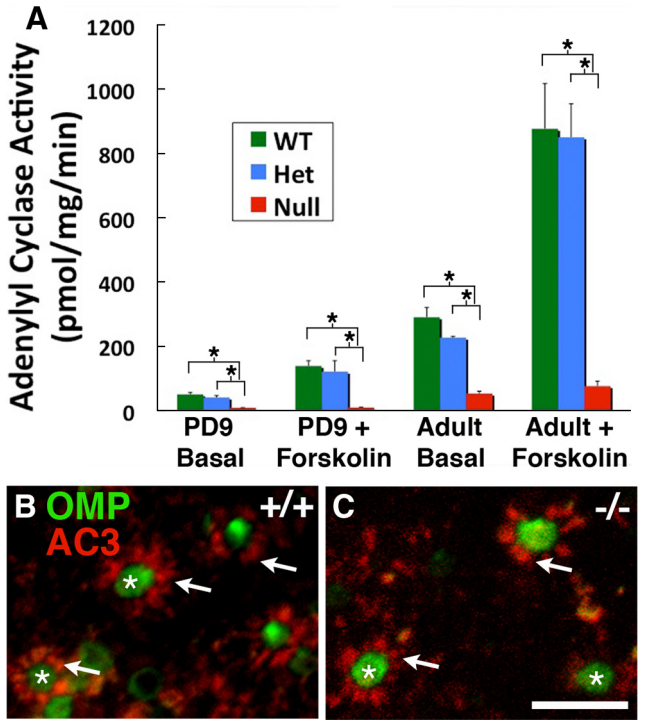


**Figure 3.** Adenylyl cyclase activity is significantly decreased in *β3GnT2*$^{-/-}$ OEs. ***A***, OE homogenates from WT, heterozygous (Het), and β3GnT2 null mice were assayed for adenylyl cyclase activity in the presence of 10 μM forskolin, an activator of adenylyl cyclases, or DMSO control (basal) by measuring cAMP production. Levels of adenylyl cyclase activity were extremely low in all null samples tested relative to the number of AC3-expressing OSNs that persist in the *β3GnT2*$^{-/-}$ OE. Statistics: Student's *t* test, $*p < 0.05$, mean ± SEM ($n = 3$). Differences between WT and Het samples in each group were not significant. ***B***, ***C***, High magnification. *En face* view of OMP$^{+}$ OSN dendritic knobs (asterisks) and AC3$^{+}$ sensory cilia (arrows). The loss of PLN glycans has no obvious effects on the ability of AC3 to localize to cilia. Scale bar, 5 μm.

### β3GnT2 modifies AC3 with PLN

We next investigated the effect of β3GnT2 loss on AC3 glycosylation and expression. In the OE of β3GnT2 WT mice, the spectrum of LEA-reactive glycoproteins is visible on Western blots as a diffuse high molecular weight smear. In contrast, LEA$^{+}$ glycans are absent from the OE of *β3GnT2*$^{-/-}$ mice, confirming that PLN synthesis in OSNs is exclusively β3GnT2 dependent (Fig. 2*A*, lanes 1, 2). The most heavily glycosylated form of AC3 runs diffusely at an unusually high molecular weight relative to its 129 kDa polypeptide size. This low mobility may reflect the aberrant migration of highly glycosylated proteins on polyacrylamide gels due to poor binding of SDS to neutral oligosaccharides (Leach et al., 1980). Consistent with this, AC3 from the null OE runs at 140 kDa, much closer to its predicted molecular mass, as a result of the loss of PLN from residual core glycan chains (Fig. 2*A*, lanes 3, 4). In addition, AC3 protein is decreased in the null OE, which could reflect an effect of PLN on AC3 expression or the known loss of mature OSNs in *β3GnT2*$^{-/-}$ mice (Henion et al., 2005).Together, these data show that PLN is a major constituent of AC3 glycosylation that may be required for AC3 stability or neuronal survival.

Other olfactory glycoproteins are not as significantly altered in *β3GnT2*$^{-/-}$ mice. In the rat OE, NCAM is modified with lactosamine-based carbohydrates that have been suggested to influence axon sorting (Storan et al., 2004). The NCAM-180 isoform that is partially retained on LEA-agarose (Fig. 1*F*) is only moderately reduced in expression, whereas NCAM-140 is un-

changed (Fig. 2*A*, lanes 5, 6). Neither NCAM isoform shifts position significantly on gels, indicating that PLN is a minor component of NCAM glycosylation.

To examine the nature of AC3 glycosylation in more detail, we incubated OE homogenates from WT and *β3GnT2*$^{-/-}$ OEs with PNGase F to remove *N*-glycans and analyzed AC3 migration by Western blotting. PNGase F treatment of WT OE lysates restored the mobility of most high molecular weight AC3 to its calculated molecular mass near 129 kDa (Fig. 2*B*, lanes 1, 2). Incubation of *β3GnT2*$^{-/-}$ OEs with PNGase F removes the residual *N*-glycans from the 140 kDa AC3 glycoform, also returning its mobility to that expected of the native polypeptide (Fig. 2*B*, lanes 3, 4). The PNGase F sensitivity of these glycans indicates that the heterogeneous migration of AC3 results from PLN modifications that are *N*-linked and not from mucin-type *O*-glycans. Furthermore, AC3 from *β3GnT2*$^{-/-}$ OEs still contains residual *N*-linked glycans that may be required for trafficking through the endoplasmic reticulum and Golgi and transport to the plasma membrane.

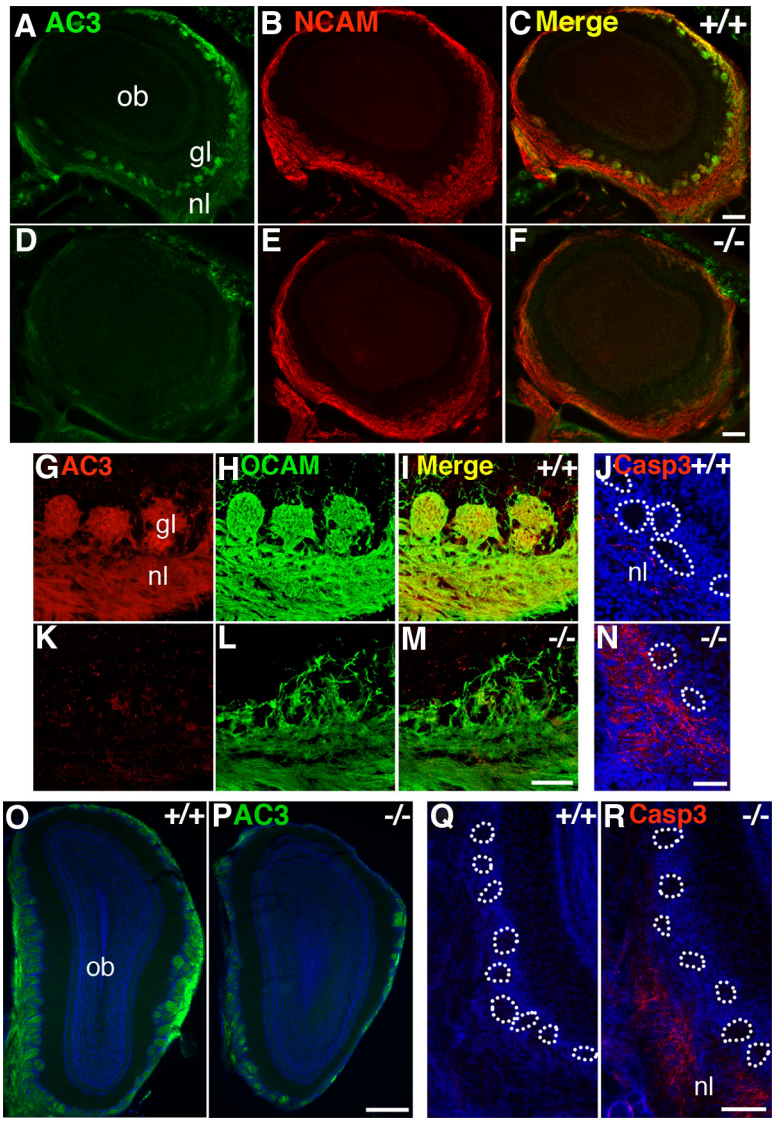


**Figure 4.** AC3 expression is decreased in the postnatal OB of null mice. ***A–C***, Immunocytochemical colocalization of AC3 (green) with the axonal marker NCAM (red) in PD3 OBs. AC3 localizes to axons in the nerve layer (nl) surrounding the OB (ob) and is particularly heavily expressed in glomeruli (gl). Scale bar, 100 μm. ***D–F***, In *β3GnT2*$^{-/-}$ mice AC3 expression is lost from the OB nerve layer. Few glomeruli form in the null OB at this age. Scale bar, 100 μm. ***G–I***, Confocal imaging of AC3 expression (red) in the PD7 WT OB. The axonal marker OCAM (green) colocalizes with AC3 in all olfactory axons in the ventral OB. ***J***, Immunoreactivity for caspase-3 (red) shows few degenerating fibers in the nerve layer and glomeruli (dotted circles) of the WT OB. ***K–M***, Although OCAM$^{+}$ fibers (green) innervate the nerve layer and aberrant glomeruli of PD7 *β3GnT2*$^{-/-}$ OBs, they fail to express AC3 (red). Scale bar, 50 μm for ***G–I***, ***K–M***. ***N***, Caspase-3 immunoreactivity associated with OSN cell death is dramatically increased in the null OB nerve layer. Scale bar, 50 μm for ***J***, ***N***. ***O***, ***P***, AC3 immunoreactivity in the adult olfactory bulb (ob). AC3 (green) is expressed at reduced levels in the disorganized glomeruli of *β3GnT2*$^{-/-}$ mice despite the absence of AC3 activity in OSNs. Scale bar, 400 μm. ***Q***, ***R***, Axonal degeneration is ongoing in the nerve layer of adult null mice as detected by activated caspase-3 (red) expression. Scale bar, 100 μm. Nuclei are labeled with Draq5 (blue).

### AC3$^{+}$ OSNs are specifically lost from *β3GnT2*$^{-/-}$ OEs

We next immunolabeled AC3 neurons in WT and *β3GnT2*$^{-/-}$ OEs to investigate how PLN loss affects OSN survival. In PD3 WT OEs, AC3 accumulates in the apical compartment of OSN cell bodies and is also highly concentrated in sensory cilia, forming a dense mat of labeling at the luminal surface of the nasal cavity (Fig. 2*C*). In the null OE, there is a significant decrease in the number of AC3$^{+}$ neurons, although the level of AC3 expression per cell appears similar to that in WTs (Fig. 2*D*). The decrease in AC3$^{+}$ OSNs is further supported by a similar loss of *AC3*-expressing neurons in null OEs by *in situ* hybridization (Fig. 2*C*′,*D*′). Likewise, the number of neurons expressing OMP, a marker of functionally mature OSNs, is reduced to a similar degree to that of AC3 (Fig. 2*E*,*F*). Conversely, immature OSNs expressing the marker GAP-43 are moderately increased in the nulls (Fig. 2*E*,*F*), while *NeuroD1*-expressing neural precursors appeared unchanged (Fig. 2*E*′,*F*′). Thus, the effects of β3GnT2 ablation appear specific to differentiated neurons and are not a downstream consequence of OSN precursor loss.

The decrease in AC3$^{+}$ neurons persists in adult mice. In WT animals, the number of AC3$^{+}$ neurons is greatly expanded relative to PD3, as the OE becomes increasingly composed of differentiated OSNs (Fig. 2*G*). In adult β3GnT2$^{-/-}$ mice there is also a significant increase in the number of AC3$^{+}$ OSNs compared to PD3, although this number is still reduced relative to WT littermates (Fig. 2*H*). Quantification of these decreases reveals that AC3$^{+}$ OSNs in PD3 nulls are reduced 58% compared to WT controls ($n = 4$, $p < 0.001$), a ratio that is maintained in adults (Fig. 2*I*). Relative expression levels for *AC3*, *OMP*, and *GAP-43*, determined by qPCR, further confirm that it is the mature OSN population that is affected by β3GnT2 loss in adults (Fig. 2*J*).

### AC3 activity is significantly decreased in β3GnT2$^{-/-}$ mice

To investigate the potential effects of PLN loss on cAMP generation, we examined basal and forskolin-stimulated adenylyl cyclase activity in WT and *β3GnT2*$^{-/-}$ OEs. Despite the fact that nearly half of AC3$^{+}$ OSNs persist in null mice, adenylyl cyclase

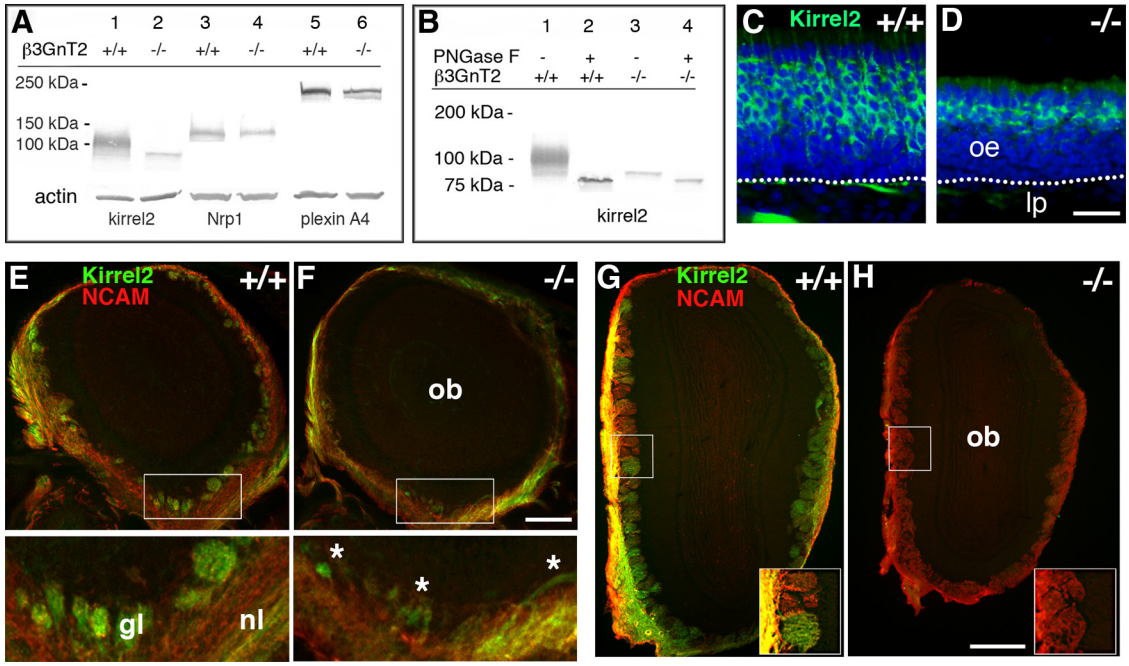


**Figure 5.** Kirrel2 expression in the adult OB is β3GnT2 dependent. ***A***, Western blot analysis of OE preparations from adult WT and *β3GnT2*$^{-/-}$ mice. Kirrel2 is heavily modified with PLN glycans, but Nrp1 is not directly glycosylated by β3GnT2. Only a small portion of plexin-A4 is β3GnT2 modified. ***B***, PNGase F digestion of OE lysates reveals that kirrel2 glycosylation is exclusively *N*-linked. ***C***, ***D***, The number of kirrel2 immunoreactive OSNs (green) is reduced in the olfactory epithelium (op) of adult null mice. Nuclei are labeled with Draq5 (blue). lp, Lamina propria. Scale bar, 25 μm. ***E***, ***F***, Kirrel2 (green) and NCAM (red) are coexpressed by most glomeruli in the PD3 OB. Although few glomeruli form in PD3 *β3GnT2*$^{-/-}$ OBs, these still express kirrel2 (asterisks). Bottom panel shows detail of boxed region. gl, Glomeruli, nl, nerve layer. Scale bar, 100 μm. ***G***, ***H***, Kirrel2 is mosaically expressed in the adult olfactory bulb (ob) of WT mice (see inset) but is completely absent from the OB of *β3GnT2*$^{-/-}$ mice. Scale bar, 200 μm.

enzymatic activity was extremely low (Fig. 3*A*). The basal level of cAMP production was ~6-fold higher in the PD9 WT OE (cAMP generated in pmol/mg/min ± SE; WT, 50.13 ± 5.2; null, 8.2 ± 0.4). Forskolin stimulation elevated adenylyl cyclase activity over 5-fold in the null, although the amount of cAMP generated was still <20% that of WT littermates (WT, 290 ± 30; null, 52.7 ± 7.1). Adenylyl cyclase activity in adult null mice, although higher than at PD9, was still extremely low, even with forskolin stimulation (WT, 876.7 ± 141; null, 75.8 ± 15.6). Heterozygous mice displayed consistently reduced adenylyl cyclase activity compared to WT controls, although this difference was not significant. Together, these results suggest that AC3$^{+}$ OSNs that persist in the OE of mutant mice are deficient in their ability to generate cAMP.

The reason for AC3 activity loss does not appear to involve defective trafficking of AC3 to cilia. High-magnification *en face* scans across the surface of the OE reveals apparently normal localization of AC3 protein to the multiple cilia proximal segments that surround the dendritic knob (Fig. 3*B*,*C*). Additionally, there is no obvious decrease in labeling intensities in either cilia or OSN cell bodies, except for the lower number of labeled OSNs in the OE of null mice. It thus appears that PLN glycans influence AC3 enzyme activity without affecting protein expression or trafficking to cilia.

### AC3 is absent from early postnatal *β3GnT2*$^{-/-}$ OB projections

In addition to olfactory signal transduction, cAMP levels influence the site of glomerular synapse formation in the OB by regulating transcription of axon guidance molecules (Imai et al., 2006; 2009). Recently, it has become clear that AC3 protein is expressed not only in OSN cell bodies and cilia but is also present on axons (Dal Col et al., 2007; Zou et al., 2007). In PD3 WT mice, AC3 colocalizes completely with the axonal marker NCAM in all glomeruli (Fig. 4*A*–*C*). Importantly, in *β3GnT2*$^{-/-}$ mice where glomerular formation is delayed (Henion et al., 2005), AC3 is absent from olfactory axons. Even residual fibers within the nerve layer that are strongly labeled with NCAM fail to express AC3 (Fig. 4*D*–F).

To visualize this loss more closely, OBs were immunolabeled with the axonal marker OCAM at PD7, after glomeruli have emerged in WT (Fig. 4*G*–*I*), but not *β3GnT2*$^{-/-}$ OBs (Henion et al., 2005). Despite the delay in glomerular formation, many OCAM-expressing axons are still present in the nerve layer of mutant mice. However, unlike their WT littermates, these axons fail to express AC3 (Fig. 4*K*–*M*). There is also a dramatic increase in activated caspase-3 reactivity associated with degenerating olfactory axons in the mutant nerve layer (Fig. 4, compare *J*, *N*). Thus, the elimination of many OSNs occurs at a late stage of development, concurrent with or shortly after axons attempt to form synaptic contacts. OSN cell death is one consequence of the loss of trophic support from the absence of OB connectivity (Carr and Farbman, 1992). These results are also consistent with the finding that some OR reporter-labeled axons initially form protoglomeruli in the *β3GnT2*$^{-/-}$ OB but are subsequently eliminated in adults (Henion et al., 2005).

Although AC3 null mice do not exhibit electroolfactogram responses to odorants, their axons still exit the nerve layer and form rudimentary glomeruli (Wong et al., 2000, Trinh and Storm, 2003; Dal Col et al., 2007; Zou et al., 2007). *β3GnT2*$^{-/-}$ mice display a similarly disorganized glomerular layer in the absence of AC3 activity that persists in adults (Henion et al., 2005; Schwarting and Henion, 2007). The ability of null mice to discriminate AC3-dependent odors is also moderately reduced rel-

ative to WT controls, although they are not anosmic (Henion et al., 2005; T. K. Knott, G. A. Schwarting, unpublished data). In adults, after an initial early postnatal delay, AC3 is eventually expressed on null olfactory axons within the nerve layer and glomeruli, although the levels remain below those of WT controls (Fig. 4*O*,*P*). Activated caspase-3 expression also remains elevated in the adult nerve layer (Fig. 4*Q*,*R*) and OE (data not shown), indicating that cell death is an ongoing process in the *β3GnT2*$^{-/-}$ OE, where AC3 activity is severely decreased despite the presence of AC3 protein.

### Misregulation of cAMP-dependent guidance cues in β3GnT2$^{-/-}$ mice

LEA lectin blotting identified several olfactory axon guidance molecules that are also modified by PLN glycans (Fig. 1*F*). We investigated whether the expression of any of these is altered in *β3GnT2*$^{-/-}$ mice similarly as that of AC3 using Western blot analysis. Kirrel2, an activity-dependent immunoglobulin superfamily glycoprotein (Serizawa et al., 2006), runs on gels as a broad 100 kDa band (Fig. 5*A*, lanes 1, 2). In mutant OEs, kirrel2 migrated at 90 kDa due to a decrease in β3GnT2-dependent glycosylation. In addition, kirrel2 protein levels were also decreased. PNGase F treatment considerably reduces the size heterogeneity of WT kirrel2, resulting in a sharply migrating 75 kDa protein that approximates its calculated molecular mass (Fig. 5*B*). Kirrel2 blotted from *β3GnT2*$^{-/-}$ OEs migrates as a homogeneous 90 kDa band, consistent with the presence of residual *N*-glycan core-structures. PNGase F treatment of mutant kirrel2 returns its size to 75 kDa, identical to that in the WT. Thus, much like AC3, kirrel2 is modified by *N*-linked PLN glycans that contribute significantly to the variable migration of these glycoproteins on gels.

The receptor complex for Sema3A is a dimer composed of Nrp1 and plexin-A4 (Suto et al., 2005). Nrp1 is a 103 kDa single pass transmembrane protein with several potential *N*- and *O*-linked glycosylation sites. By Western blot analysis, Nrp1 migrates as a 140 kDa protein in WT OEs, which does not change in nulls (Fig. 5*A*, lanes 3, 4). Plexin-A4 is a 212 kDa single pass transmembrane glycoprotein that migrates as a major 240 kDa band and a faint 230 kDa band. In null mice, the 240 kDa band is modestly decreased while the 230 kDa band is increased from the loss of PLN (Fig. 5*A*, lanes 5, 6). PNGase F digestion further confirmed that these modifications were carried on *N*-glycan chains (data not shown).

A decrease in kirrel2 expression in mutant mice is also evident by an overall reduction in the number of OSNs expressing this adhesion molecule. In the WT OE, kirrel2 is expressed by most mature neurons but is decreased in mutants to only a few layers of cells in the most apical OE regions (Fig. 5*C*,*D*). In the OB, kirrel2 is broadly expressed at PD3 but refines in adults to a variable pattern of glomerular innervation, with the majority being positive to some degree (Fig. 5*E*,*G*). The mosaic expression of kirrel2 by different axon subsets has been proposed to mediate local axon sorting into glomeruli (Serizawa et al., 2006). How-

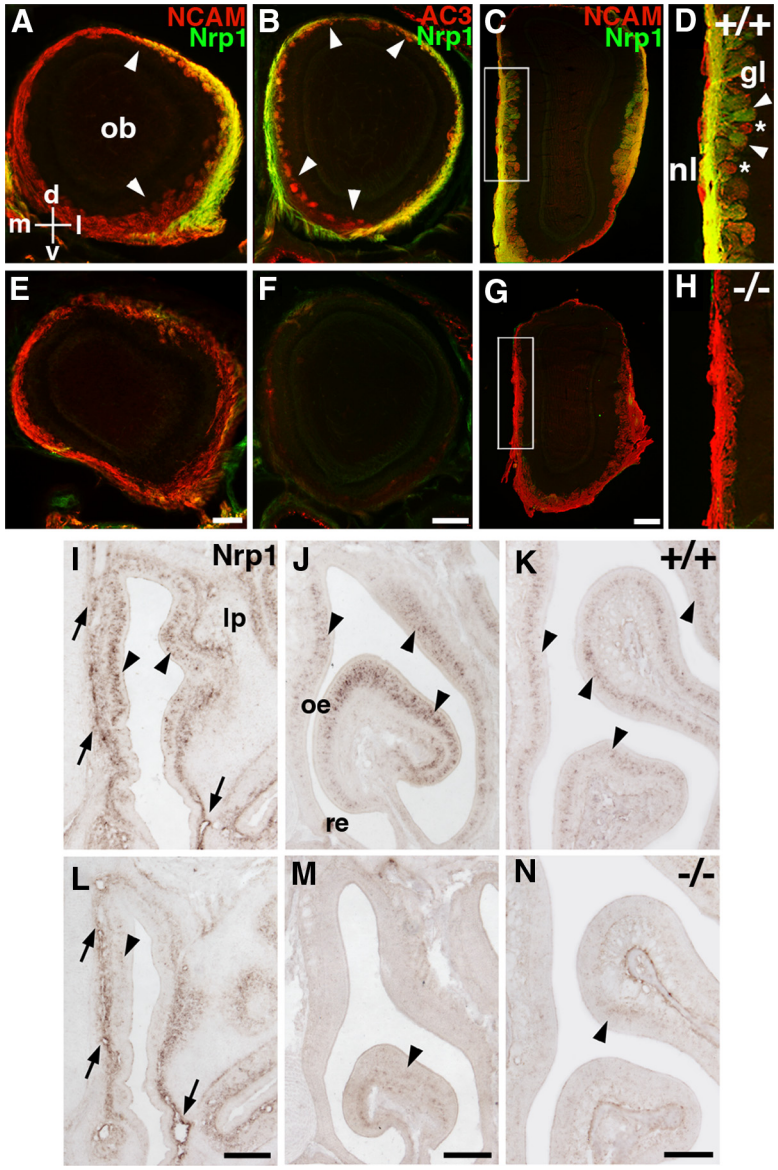


**Figure 6.** Reduced expression of Nrp1 in *β3GnT2*$^{-/-}$ mice. ***A***, In the anterior olfactory bulb (ob) of PD3 WT mice, Nrp1$^{+}$ axons (green) are routed to lateral OB domains (region between arrowheads). Medial (m), lateral (l), dorsal (d), and ventral (v) domains are shown and apply to all. ***B***, In the posterior OB, medial and lateral domains of PD3 WT mice are innervated by Nrp1$^{+}$ axons (green), although almost all glomeruli express AC3 (red). ***C***, ***D***, This expression is maintained in adult mice, although Nrp1 refines to a mosaic pattern. The boxed region in ***C*** is shown in detail in ***D***. Some glomeruli (gl) express Nrp1 at high levels (arrowheads) while others are negative (asterisks). nl, Nerve layer. ***E***, Nrp1 is absent from NCAM-expressing axons in the anterior OB of PD3 *β3GnT2*$^{-/-}$ mice. Scale bar, 100 μm. ***F***, Both AC3 and Nrp1 are absent from the posterior OB of PD3 *β3GnT2*$^{-/-}$ mice. Scale bar, 200 μm. ***G***, ***H***, Nrp1 is not re-expressed by NCAM$^{+}$ axons innervating glomeruli in the adult OB, in contrast to AC3 (see Fig. 4*P*), consistent with decreased levels of cAMP synthesis. Boxed region in ***G*** is shown in detail in ***H***. Scale bar, 300 μm. ***I–N***, *In situ* hybridization analysis of Nrp1 mRNA expression at embryonic day 18 (***I***, ***L***), PD9 (***J***, ***M***), and PD22 (***K***, ***N***) in WT (***I***, ***K***) and β3GnT2$^{-/-}$ mice (***L–N***). Nrp1 is strongly expressed by many OSNs in the olfactory epithelium (oe) (arrowheads) and in blood vessels (arrows), but is absent from the respiratory epithelium (re). In null mice, Nrp1 expression in the OE is significantly decreased, although the level of Nrp1 mRNA in blood vessels is unaffected. lp, Lamina propria. Scale bar, 200 μM for (***I–N***).

ever, kirrel2 expression is progressively lost with age in null mice. Although there are few glomeruli in the PD3 null OB, there is expression of kirrel2 on olfactory axons within the nerve layer and the few protoglomeruli that form (Fig. 5*F*). In adults, kirrel2 is completely absent from all fibers in both the mutant nerve layer and glomeruli, consistent with the decrease in AC3 activity in null mice (Fig. 5*H*).

Nrp1 plays a critical role in olfactory axon targeting through repulsive interactions with the secreted ligand Sema3A, expressed by glial ensheathing cells within the ventral OB nerve layer and subsets of OSNs (Pasterkamp et al., 1998; Schwarting et al., 2000; Imai et al., 2009). Nrp1 levels in OSNs are regulated by cAMP determined through AC3 (Dal Col et al., 2007; Imai et al., 2006; 2009; Miller et al., 2010). Expression of Nrp1 is decreased in the *β3GnT2*$^{-/-}$ OE by Western blot analysis, although the receptor is not directly modified by PLN (Figs. 1*D*, 5*A*). This decrease may therefore in part reflect the loss of AC3-derived cAMP signals, which could be one mechanism for targeting defects observed in the null OB.

To investigate this further, we immunolabeled OBs from early postnatal and adult null mice to examine potential alterations in Nrp1 distribution. At PD3, Nrp1 expression in posterior glomeruli is restricted to medial and lateral domains, whereas AC3 is strongly expressed by virtually all protoglomeruli (Fig. 6*A*,*B*). This patterned expression is maintained in adults, although like kirrel2 its distribution is mosaic, with some glomeruli within these domains failing to express Nrp1 while others are strongly positive (Fig. 6*C*,*D*). In PD3 null mice, Nrp1 is absent from all neuronal fibers in both the nerve layer and glomeruli (Fig. 6*E*,*F*). The loss of Nrp1 expression continues in adult mutants, despite the emergence of many small, abnormally shaped glomeruli (Fig. 6*G*,*H*).

To investigate the mechanism for this decrease, we used *in situ* hybridization to examine *Nrp1* mRNA expression at different developmental time points. As reported previously, *Nrp1* is mosaically expressed in subpopulations of OSNs in most OE regions (Fig. 6*I–K*, arrowheads) (Schwarting et al., 2004). This expression is highest prenatally and during early postnatal development, although *Nrp1* continues to be transcribed in the adult OE. Nrp1 is also strongly expressed in blood vessels adjacent to the neuroepithelium, where it influences angiogenesis and blood vessel branching independently of Sema3A through its ligand $VEGF_{165}$ (Fig. 6*I*, arrows). In *β3GnT2*$^{-/-}$ mice, the expression of *Nrp1* is greatly reduced throughout the OE at all time points, although expression in blood vessels is unaffected (Figs. 6*L–N*, 7*E*). Together with the loss of AC3 activity and the absence of Nrp1 protein expression on axons, our data support a prominent role for cAMP in regulating Nrp1 expression levels in OSNs.

Sema3A is also expressed by OSNs in a pattern complimentary to that of the Nrp1 receptor, which has been proposed to be critical for pre-target sorting of olfactory axons within nerve bundles (Imai et al., 2009). Ablation of Sema3A leads to targeting abnormalities in the OB (Schwarting et al., 2000; Taniguchi et al., 2003; Imai et al., 2009). In contrast to Nrp1, Sema3A expression in OSNs is inversely correlated with cAMP levels (Imai et al., 2009). In *β3GnT2*$^{-/-}$ mice, we observed a notable increase in *Sema3A* expression by *in situ* hybridization at all time points examined (Fig. 7*A–D*). This alteration, as well as those identified for several other cAMP-dependent molecules, was confirmed by qPCR (Fig. 7*E*).

Thus, the loss of AC3 activity observed in *β3GnT2*$^{-/-}$ mice correlates with predictable alterations in multiple guidance cues and sorting molecules. These disruptions provide a mechanism for the axon guidance phenotype observed in *β3GnT2*$^{-/-}$ mice, as well as the loss of OR subsets through a

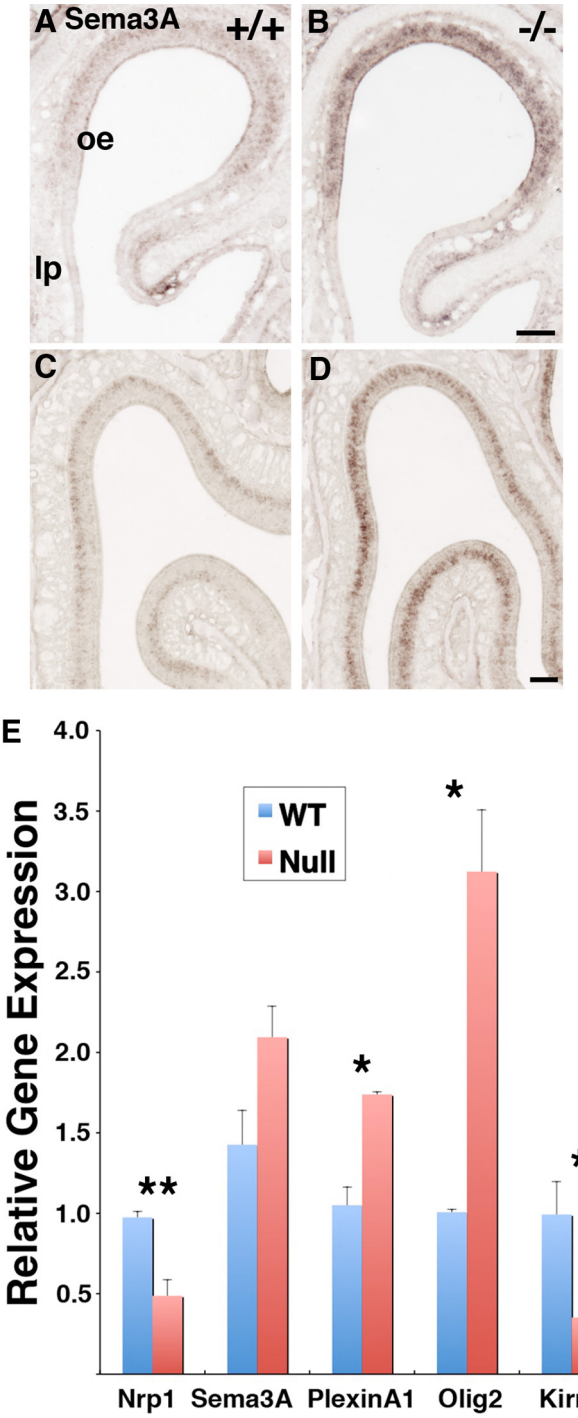


**Figure 7.** Increased expression of *Sema3A* in the *β3GnT2*$^{-/-}$ OE. ***A–D***, *In situ* hybridization analysis of *Sema3A* mRNA expression in OSNs. At both PD3 (***A***, ***B***) and PD22 (***C***, ***D***) expression levels of *Sema3A*, which are low in WT OSNs (***A***, ***C***), are markedly upregulated in β3GnT2$^{-/-}$ mice. lp, Lamina propria; oe, olfactory epithelium. Scale bars, 100 μm. ***E***, Quantitative PCR analysis for relative expression of different OSN genes previously shown to be positively (*Nrp1*, *kirrel2*) or negatively (*Sema3A*, *PlexinA1*, *Olig2*) correlated with cAMP levels (Imai et al., 2009). The results are consistent with a reduced level of cAMP signaling in *β3GnT2*$^{-/-}$ mice. Results are the average relative quantification normalized to a *RNA Polymerase 2* reference target. Statistics: Student's *t* test, $^{**}p < 0.001$, $^{*}p < 0.05$; mean ± SEM ($n = 6$ for *Nrp1*; $n = 3$ for others).

failure to form proper connections with synaptic partners in the OB.

## Discussion

Olfactory projections are patterned by multiple guidance cues that act cooperatively to target axons to stereotyped loci in the OB. The OR-dependent production of cAMP by AC3 modulates transcription of *Nrp1*, its ligand *Sema3A*, as well other genes that regulate growth cone dynamics (Imai et al., 2006, 2009). In this report, we show that β3GnT2 glycosylation influences the expression of multiple axon guidance molecules that mediate proper OB connectivity. This is achieved through the synthesis of PLN glycans on AC3, which are required for efficient cAMP production by OSNs. An additional consequence of β3GnT2 deletion is the loss of AC3 and kirrel2 from OB axons. This deficit suggests a defect in localization or maintenance of these proteins on *β3GnT2*$^{-/-}$ axons. These distinct effects of β3GnT2 loss, summarized in Figure 8, will be discussed in greater detail below.

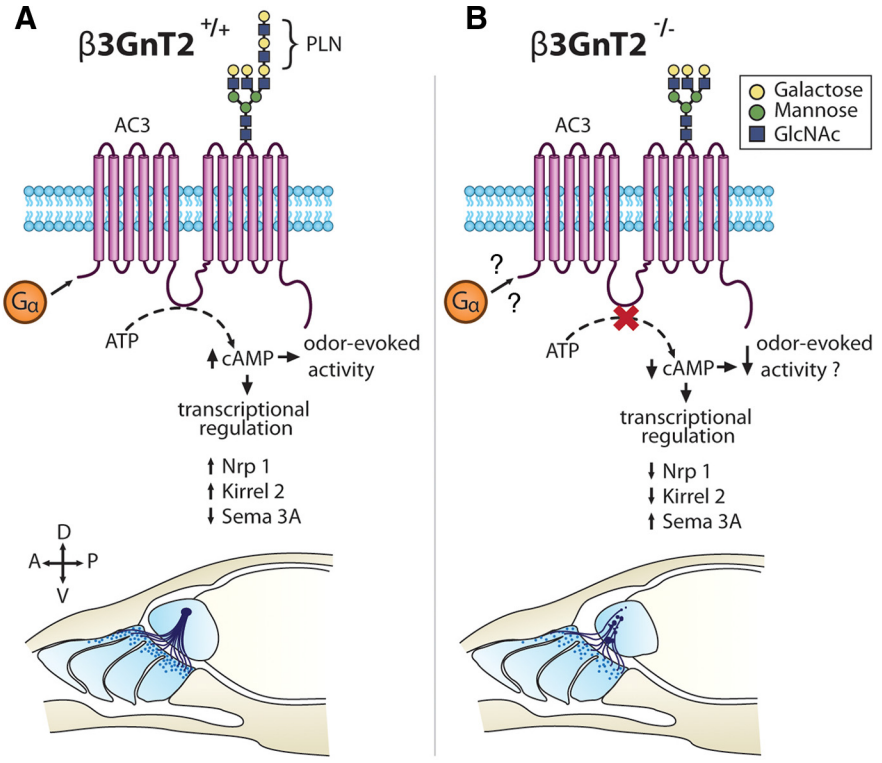


**Figure 8.** A model for β3GnT2 effects on OB innervation. ***A***, In OSNs, OR-derived cAMP signals generated by AC3 are required for odor-evoked signaling. In addition, AC3-dependent cAMP regulates the expression of the axon guidance molecules Nrp1 and Sema3A, which influence glomerular positioning in the OB (bottom panel) (Dal Col et al., 2007; Imai et al., 2006, 2009). Other adhesion molecules such as kirrel2, which may modulate local axon sorting, are also activity-dependent. β3GnT2 initiates the expression of PLN chains on AC3 that are necessary for enzymatic activity. ***B***, In *β3GnT2*$^{-/-}$ mice, cAMP levels are dramatically decreased in parallel with Nrp1 and kirrel2, while Sema3A expression is increased. The mechanism by which β3GnT2 influences AC3 activity is currently unclear. PLN could be required for AC3 enzymatic activity directly. Alternatively, PLN could mediate the formation of complexes that promote G protein coupling and downstream signaling. A second consequence of β3GnT2 deletion that may be independent from OSN signaling is the loss of AC3 from axons. The absence of either β3GnT2 or AC3 leads to similar OB innervation defects, including the formation of multiple heterotypic glomeruli by M72 axons that are ectopically located in the anterior OB (bottom panel) (Chesler et al., 2007; Schwarting and Henion, 2007). Adult *β3GnT2*$^{-/-}$ mice are not anosmic, and exhibit apparently milder deficits in olfactory performance relative to *AC3*$^{-/-}$ mice (Wong et al., 2000; Trinh and Storm, 2003; Henion et al., 2005).

### β3GnT2 glycosylation is essential for AC3 activity

Although β3GnT2 modifies a number of glycoproteins, many of the defects associated with PLN loss appear to result from decreased AC3 activity. The phenotypes for *AC3*$^{-/-}$ and *β3GnT2*$^{-/-}$ mice, each characterized by a deficit in cAMP production, are strikingly similar (Trinh and Storm, 2003; Henion et al., 2005; Dal Col et al., 2007; Zou et al., 2007): (1) the formation of disorganized glomeruli that are largely excluded from the dorsal OB; (2) identical defects in axon guidance and OSN survival for several representative OR subsets; (3) a persistence of heterotypic glomeruli that lasts into adulthood; and (4) the loss of cAMP-dependent proteins, Nrp1 and kirrel2, and the upregulation of Sema3A. This overlapping spectrum of defects strongly suggests that β3GnT2 is necessary for maintaining the AC3-dependent cAMP levels required for olfactory map formation.

In *β3GnT2*$^{-/-}$ mice, forskolin-stimulated AC3 activity is reduced 80–90% in the OE (Fig. 3*A*). Although AC2, AC3, and AC4 are expressed in the OE, *AC3*$^{-/-}$ mice are functionally anosmic and fail to elicit behavioral or electrophysiological responses to a variety of odorants (Wong et al., 2000; Trinh and Storm, 2003). These studies identified AC3 as the only adenylyl cyclase that signals downstream of odorant receptor activation. Interestingly, *AC3*$^{-/-}$ mice exhibit higher residual cAMP responses to forskolin than *β3GnT2*$^{-/-}$ mice, presumably from the activity of these residual isoforms. Like AC3, AC2 is a heavily glycosylated glycoprotein (Wong et al., 2000). It is possible that PLN may be important for AC2 activity as well. All nine mammalian adenylyl cyclases share conserved *N*-glycosylation sites within extracellular loops 5 and/or 6, suggesting that these glycans may be important for protein expression or function (Wu et al., 2001).

It is unclear at present why PLN modifications are critical for cAMP synthesis. Complete removal *of N*-glycosylation can lead to protein retention in the endoplasmic reticulum (Helenius and Aebi, 2001). However, β3GnT2 acts distally on *N*-glycan branches, and its ablation leaves intact *N*-glycan core structures required for folding and transport (Fig. 2*B*). In addition, AC3 localizes normally to the cilia plasma membrane (Fig. 3*B*,*C*). Although it is possible that PLN could be required for AC3 enzymatic activity directly, *in vitro* experiments examining the effects of prematurely blocking AC3 glycan extensions would not appear to support such a role (Li et al., 2007).

A possible mechanism by which β3GnT2 could promote cAMP production would be to facilitate the formation of signaling complexes through PLN interactions with endogenous lectins in the extracellular matrix. Within cellular microdomains, specificity needs to be provided to cAMP signals to promote localized responses. The $\beta_2$-adrenergic receptor, for example, associates with adenylyl cyclases and the $Ca_v1.2$ channel in a complex that promotes "fight or flight" responses (Davare et al., 2001). PLN could enhance the association of AC3 with other signaling proteins to amplify OR-derived stimulation. We have previously shown that the PLN binding proteins galectins-1 and -9 are highly expressed along axon tracts between the OE and OB (Ma-

hanthappa et al., 1994; Schwarting et al., 2000). These galectins have functionally multivalent binding sites that could crosslink AC3 with other signaling proteins, holding these molecules in close proximity at the cell surface.

### β3GnT2 maintains AC3 on olfactory axons

An issue that complicates our understanding of the role of activity in olfactory targeting is the fact that all proteins required for odorant signaling, including AC3, ORs, $G_{\alpha}$s, and CNGA2, are expressed not only in cilia but also in axon termini, where they can mediate cAMP production and $[Ca^{2+}]$ influx (Maritan et al., 2009). How cAMP levels in cilia are coordinated with axonal signaling components, particularly in the absence of obvious sources of distal ligand stimulation, is not known. Intrinsic OR signaling in growth cones has been proposed as a potential mechanism for establishing cAMP levels in different axon subsets (Imai and Sakano, 2008).

It is noteworthy, therefore, that AC3 is initially absent from axons that innervate the OB in embryonic and early postnatal *β3GnT2*$^{-/-}$ mice. How this loss is related to the decreased cAMP synthesis we measured in null OSNs is unclear, but it may be critical to the targeting defects observed in mutants. It is possible, for example, that cAMP synthesized in the axonal compartment influences OSN gene expression, which could account for the loss of Nrp1 and kirrel2 from *β3GnT2*$^{-/-}$ projections. Focal exposure of olfactory growth cones to odorants has been shown to mediate cAMP production, nuclear protein kinase A translocation, and potentially gene transcription (Maritan et al., 2009). However, a definitive role for localized growth cone signaling in olfactory axon targeting remains to be shown experimentally. In adults, AC3 is detectable at low levels on null axons within the nerve layer and glomeruli, suggesting potentially a permissive role in OB reinnervation (Fig. 4*O*,*P*). Despite this, cAMP production remains dramatically reduced in *β3GnT2*$^{-/-}$ OEs, and Nrp1 and kirrel2 are absent from adult null axons. Furthermore, elevated levels of axon degeneration are detectable in the null OB throughout adulthood, making the significance of this delayed AC3 expression unclear.

There are several mechanisms by which β3GnT2 could promote axonal localization of AC3 and kirrel2. PLN may be required for axonal transport or to directly maintain glycoprotein surface expression through interactions with carbohydrate binding proteins in the extracellular matrix. Both AC3 and kirrel2 are heavily modified by PLN, and the high molecular weight glycoforms of each are specifically decreased in β3GnT2 mutants. Olfactory axons are exposed to galectin-1 and -9, which are produced by glial cells along axonal pathways between the OE and OB (Crandall et al., 2000). Thus, in addition to the requirement for PLN in AC3 activity, β3GnT2 glycosylation could also function directly to promote axon localization.

Kirrel2 expression has also been reported to be upregulated by neuronal activity that requires CNGA2 (Serizawa et al., 2006). Expression levels of activity-regulated genes may also vary depending on stimulation within the local odor environment (Bennett et al., 2010). The severe decrease in cAMP levels in the *β3GnT2*$^{-/-}$ OE suggests that odor-evoked activity would be compromised, which could account for the loss of kirrel2 from OSNs. *β3GnT2*$^{-/-}$ mice, however, appear to have only moderately affected behavioral responses to AC3-dependent odorants, suggesting significant residual olfactory function (Henion et al., 2005; T. K. Knott, G. A. Schwarting, unpublished data). This is surprising given the central role of cAMP in odor-evoked activity. The influx of $[Ca^{2+}]$ in stimulated OSNs occurs on timescales much faster than those for cAMP accumulation (Maritan et al., 2009), perhaps suggesting that neuronal activity could be less sensitive than cAMP-dependent gene expression to the decreased activity of AC3 in the *β3GnT2*$^{-/-}$ OE.

### β3GnT2 function in axon guidance

The increased expression of Sema3A by OSNs and the loss of Nrp1 from axons that reach the OB appear to be critical aspects of the mistargeting in *β3GnT2*$^{-/-}$ mice. The importance of Nrp1-Sema3A repulsive interactions for glomerular positioning is clear from the guidance defects observed in *Sema3A*$^{-/-}$ mice (Schwarting et al., 2000, 2004; Taniguchi et al., 2003) and in transgenic models with altered Nrp1 expression (Imai et al., 2009). Manipulating levels of cAMP also alters the expression of Nrp1 in OSNs of transgenic mice (Imai et al., 2006, 2009). Furthermore, when AC3 activity is ablated, Nrp1 expression is lost from axons (Dal Col et al., 2007; Miller et al., 2010).

In early postnatal *β3GnT2*$^{-/-}$ mice with very low levels of AC3 activity, Nrp1 is likewise absent from projections to the OB. This decrease is not a direct consequence of the loss of glycosylation, since Nrp1 is not a substrate for β3GnT2. Rather, the large decrease in *Nrp1* mRNA expression, detected both by *in situ* hybridization and qPCR at all developmental time points, points toward a failure in cAMP-dependent transcriptional activation. In the absence of β3GnT2-dependent cAMP signaling, a significant number of M72 axons mistarget to the anterior OB, consistent with *AC3*$^{-/-}$ mice and transgenic models where Nrp1 levels are decreased (Fig. 8) (Chesler at al., 2007; Imai et al., 2009).

Unlike other sensory systems where axons respond to uniform gradients of guidance cues in target tissues, olfactory axon targeting is achieved in part by the relative levels of guidance and cell adhesion molecules expressed mosaically by subsets of OSNs and their axons (Cutforth et al., 2003; Schwarting et al., 2000, 2004; Schwarting and Henion, 2008; Serizawa et al., 2006). Nrp1 itself is not expressed in a linear gradient in the OB (Schwarting et al., 2004). Even in posterior OB domains with elevated expression, Nrp1 levels are highly variable among neighboring glomeruli (Fig. 6D). Other activity-dependent guidance molecules, such as plexin-A1, have been identified that might also influence axon sorting (Imai et al., 2009). Expression of this coreceptor is upregulated by low cAMP levels, as was also found for *β3GnT2*$^{-/-}$ mice (Fig. 7). It seems likely that additional guidance cues will be required for establishing glomerular positions along the anterior–posterior axis.

## References

Bakalyar HA, Reed RR (1990) Identification of a specialized adenylyl cyclase that may mediate odorant detection. Science 250:1403–1406.

Bennett MK, Kulaga HM, Reed RR (2010) Odor-evoked gene regulation and visualization in olfactory receptor neurons. Mol Cell Neurosci 43:353–362.

Biellmann F, Henion TR, Bürki K, Hennet T (2008) Impaired sexual behavior in male mice deficient for the beta1–3 *N*-acetylglucosaminyltransferase-I gene. Mol Reprod Dev 75:699–706.

Carr VM, Farbman AI (1992) Ablation of the olfactory bulb up-regulates the rate of neurogenesis and induces precocious cell death in olfactory epithelium. Exp Neurol 115:55–59.

Chesler AT, Zou DJ, Le Pichon CE, Peterlin ZA, Matthews GA, Pei X, Miller MC, Firestein S (2007) A G protein/cAMP signal cascade is required for axonal convergence into olfactory glomeruli. Proc Natl Acad Sci U S A 104:1039–1044.

Crandall JE, Dibble C, Butler D, Pays L, Ahmad N, Kostek C, Püschel AW, Schwarting GA (2000) Patterning of olfactory sensory connections is mediated by extracellular matrix proteins in the nerve layer of the olfactory bulb. J Neurobiol 45:195–206.

Cutforth T, Moring L, Mendelsohn M, Nemes A, Shah NM, Kim MM, Frisén

J, Axel R (2003) Axonal ephrin-As and odorant receptors: coordinate determination of the olfactory sensory map. Cell 114:311–322.
Dal Col JA, Matsuo T, Storm DR, Rodriguez I (2007) Adenylyl cyclase-dependent axonal targeting in the olfactory system. Development 134:2481–2489.
Davare MA, Avdonin V, Hall DD, Peden EM, Burette A, Weinberg RJ, Horne MC, Hoshi T, Hell JW (2001) A beta2 adrenergic receptor signaling complex assembled with the $Ca^{2+}$ channel Cav1.2. Science 293:98–101.
Feinstein P, Mombaerts P (2004) A contextual model for axonal sorting into glomeruli in the mouse olfactory system. Cell 117:817–831.
Helenius A, Aebi M (2001) Intracellular functions of *N*-linked glycans. Science 291:2364–2369.
Henion TR, Zhou D, Wolfer DP, Jungalwala FB, Hennet T (2001) Cloning of a mouse β1,3*N*-acetylglucosaminyltransferase GlcNAc(β1,3)Gal(beta 1,4)Glc-ceramide synthase gene encoding the key regulator of lacto-series glycolipid biosynthesis. J Biol Chem 276:30261–30269.
Henion TR, Raitcheva D, Grosholz R, Biellmann F, Skarnes WC, Hennet T, Schwarting GA (2005) β1,*3-N-Acetylglucosaminytransferase* 1 glycosylation is required for axon pathfinding by olfactory sensory neurons. J Neurosci 25:1894–1903.
Imai T, Sakano H (2008) Odorant receptor-mediated signaling in the mouse. Curr Opin Neurobiol 18:251–260.
Imai T, Suzuki M, Sakano H (2006) Odorant receptor-derived cAMP signals direct axonal targeting. Science 314:657–661.
Imai T, Yamazaki T, Kobayakawa R, Kobayakawa K, Abe T, Suzuki M, Sakano H (2009) Pre-target axon sorting establishes the neural map topography. Science 325:585–590.
Jenkins PM, McEwen DP, Martens JR (2009) Olfactory cilia: linking sensory cilia function and human disease. Chem Senses 34:451–464.
Kaupp UB (2010) Olfactory signalling in vertebrates and insects: differences and commonalities. Nat Rev Neurosci 11:188–200.
Kleene SJ (2008) The electrochemical basis of odor transduction in vertebrate olfactory cilia. Chem Senses 33:839–859.
Leach BS, Collawn JF Jr, Fish WW (1980) Behavior of glycopolypeptides with empirical molecular weight estimation methods. 1. In sodium dodecyl sulfate. Biochemistry 19:5734–5741.
Li W, Takahashi M, Shibukawa Y, Yokoe S, Gu J, Miyoshi E, Honke K, Ikeda Y, Taniguchi N (2007) Introduction of bisecting GlcNAc in *N*-glycans of adenylyl cyclase III enhances its activity. Glycobiology 17:655–662.
Mahanthappa NK, Cooper DN, Barondes SH, Schwarting GA (1994) Rat olfactory neurons can utilize the endogenous lectin, L-14, in a novel adhesion mechanism. Development 120:1373–1384.
Maritan M, Monaco G, Zamparo I, Zaccolo M, Pozzan T, Lodovichi C (2009) Odorant receptors at the growth cone are coupled to localized cAMP and $Ca^{2+}$ increases. Proc Natl Acad Sci U S A 106:3537–3542.
Merkle RK, Cummings RD (1987) Relationship of the terminal sequences to the length of poly-*N*-acetyllactosamine chains in asparagine-linked oligosaccharides from the mouse lymphoma cell line BW5147. Immobilized tomato lectin interacts with high affinity with glycopeptides containing long poly-*N*-acetyllactosamine chains. J Biol Chem 262:8179–8189.
Miller AM, Maurer LR, Zou DJ, Firestein S, Greer CA (2010) Axon fasciculation in the developing olfactory nerve. Neural Dev 5:20.
Mitchell KJ, Pinson KI, Kelly OG, Brennan J, Zupicich J, Scherz P, Leighton PA, Goodrich LV, Lu X, Avery BJ, Tate P, Dill K, Pangilinan E, Wakenight P, Tessier-Lavigne M, Skarnes WC (2001) Functional analysis of secreted and transmembrane proteins critical to mouse development. Nat Genet 28:241–249.
Mombaerts P, Wang F, Dulac C, Chao SK, Nemes A, Mendelsohn M, Edmondson J, Axel R (1996) Visualizing an olfactory sensory map. Cell 87:675–686.
Pasterkamp RJ, De Winter F, Holtmaat AJ, Verhaagen J (1998) Evidence for a role of the chemorepellent semaphorin III and its receptor neuropilin-1 in the regeneration of primary olfactory axons. J Neurosci 18:9962–9976.
Schwarting GA, Henion TR (2007) Lactosamine differentially affects olfactory sensory neuron projections to the olfactory bulb. Dev Neurobiol 67:1627–1640.
Schwarting GA, Henion TR (2008) Olfactory axon guidance: the modified rules. J Neurosci Res 86:11–17.
Schwarting GA, Kostek C, Ahmad N, Dibble C, Pays L, Püschel AW, (2000) Semaphorin 3A is required for normal guidance of olfactory axons in mice. J Neurosci 20:7691–7697.
Schwarting GA, Raitcheva D, Crandall JE, Burkhardt C, Püschel AW (2004) Semaphorin 3A mediated axon guidance regulates convergence and targeting of P2 odorant receptor axons. Eur J Neurosci 19:1800–1810.
Serizawa S, Miyamichi K, Takeuchi H, Yamagishi Y, Suzuki M, Sakano H (2006) A neuronal identity code for the odorant receptor-specific and activity-dependent axon sorting. Cell 127:1057–1069.
Shiraishi N, Natsume A, Togayachi A, Endo T, Akashima T, Yamada Y, Imai N, Nakagawa S, Koizumi S, Sekine S, Narimatsu H, Sasaki K (2001) Identification and characterization of three novel β1,*3-N-acetylglucosaminyltransferases* structurally related to the β1,3-galactosyltransferase family. J Biol Chem 276:3498–3507.
Storan MJ, Magnaldo T, Biol-N′Garagba MC, Zick Y, Key B (2004) Expression and putative role of lactoseries carbohydrates present on NCAM in the rat primary olfactory pathway. J Comp Neurol 475:289–302.
Suto F, Ito K, Uemura M, Shimizu M, Shinkawa Y, Sanbo M, Shinoda T, Tsuboi M, Takashima S, Yagi T, Fujisawa H (2005) Plexin-A4 mediates axon-repulsive activities of both secreted and transmembrane semaphorins and plays roles in nerve fiber guidance. J Neurosci 25:3628–3637.
Taniguchi M, Nagao H, Takahashi YK, Yamaguchi M, Mitsui S, Yagi T, Mori K, Shimizu T (2003) Distorted odor maps in the olfactory bulb of semaphorin 3A-deficient mice. J Neurosci 23:1390–1397.
Togayachi A, Kozono Y, Ishida H, Abe S, Suzuki N, Tsunoda Y, Hagiwara K, Kuno A, Ohkura T, Sato N, Sato T, Hirabayashi J, Ikehara Y, Tachibana K, Narimatsu H (2007) Polylactosamine on glycoproteins influences basal levels of lymphocyte and macrophage activation. Proc Natl Acad Sci U S A 104:15829–15834.
Trinh K, Storm DR (2003) Vomeronasal organ detects odorants in absence of signaling through main olfactory epithelium. Nat Neurosci 6:519–525.
Wang F, Nemes A, Mendelsohn M, Axel R (1998) ORs govern the formation of a precise topographic map. Cell 93:47–60.
Wei J, Zhao AZ, Chan GC, Baker LP, Impey S, Beavo JA, Storm DR (1998) Phosphorylation and inhibition of olfactory adenylyl cyclase by CaM kinase II in neurons: a mechanism for attenuation of olfactory signals. Neuron 21:495–504.
Wong ST, Trinh K, Hacker B, Chan GC, Lowe G, Gaggar A, Xia Z, Gold GH, Storm DR (2000) Disruption of the type III adenylyl cyclase gene leads to peripheral and behavioral anosmia in transgenic mice. Neuron 27:487–497.
Wu GC, Lai HL, Lin YW, Chu YT, Chern Y (2001) N-glycosylation and residues Asn805 and Asn890 are involved in the functional properties of type VI adenylyl cyclase. J Biol Chem 276:35450–35457.
Zhou D, Dinter A, Gutiérrez Gallego R, Kamerling JP, Vliegenthart JF, Berger EG, Hennet T (1999) A β-1,*3-N*-acetylglucosaminyltransferase with poly-*N*-acetyllactosamine synthase activity is structurally related to β-1,3-galactosyltransferases. Proc Natl Acad Sci U S A 96:406–411.
Zou DJ, Chesler AT, Le Pichon CE, Kuznetsov A, Pei X, Hwang EL, Firestein S (2007) Absence of adenylyl cyclase 3 perturbs peripheral olfactory projections in mice. J Neurosci 27:6675–6683.